Supporting Information

Enhanced CO Oxidationon on the CeO_2/Co_3O_4 nanojunctions derived from annealing of metal organic frameworks

Changlai Wang[a], Dongdong Wang[a], Yang Yang[a], Ren Li[a], Changle Chen[b*] and Qianwang Chen[a,c *]

[a]Department of Materials Science & Engineering, Hefei National Laboratory for Physical Science at Microscale & Collaborative Innovation Center of Suzhou Nano Science and Technology, University of Science and Technology of China, Hefei 230026, China

[b]Department of Polymer Science & Engineering, University of Science and Technology of China, Hefei 230031, China.

[c]High Magnetic Field Laboratory, Hefei Institutes of Physical Science, Chinese Academy of Sciences, Hefei 230031, China

* Corresponding author

Material synthesis

The Co_3O_4 used as reference was obtained by directly carbonization of $Co_3[Co(CN)_6]_2$. The typical synthetic experiments of $Co_3[Co(CN)_6]_2$ were carried out as follows: Solution A: $Co(CH_3COO)_2 \cdot nH_2O$ (0.075 mmol, 18.7 mg) was dissolved in H_2O (10 mL) under agitated stirring to obtain a transparent red solution. Solution B: $K_3[Co(CN)_6]_2$ (16.6 mg, 0.05 mmol) and PVP surfactant (0.3 g) were dissolved in distilled water (10 mL). Solution A was slowly and regularly added to solution B through a syringe to form a red colloid solution. The whole reaction was performed at room temperature with agitated stirring. After 10 min, the reaction was aged for 24 h at room temperature without any interruption. The resulting pink-colored precipitate was filtered and washed several times with distilled water and finally dried in air at 60 ℃.

Calculation method

The calculations were based on density functional theory by using the Vienna

Ab-initio Simulation Package (VASP)[1, 2]. The core electrons were replaced by the projector augmented wave pseudopotentials and the valence electrons were described by plane wave basis sets[3, 4]. The electron−electron exchange and correlation functional was used the generalized gradient approximation (GGA) [5]method with Perdew-Burke-Ernzerhof (PBE) [6]functional. To ensure the accuracy of the calculated results, the cutoff energy was set to 400 eV for the plane-wave expansion of the electronic wave function. All structures were optimized with a convergence criterion of 1×10^{-5} eV for the energy and 0.01 eV/Å for the forces. Brillouin-zone integration was performed with 5 × 5 × 1 Monkhorst-Pack grid. The adsorption energy of the CO molecule was evaluated from:

$$E_{ads} = E_{tol} - (E_{co} + E_{sur})$$

Where E_{tot}, E_{co} and E_{sur} are the energy of the total adsorbed system, CO molecule in the gas phase and the relaxed clean catalyst surface, respectively.

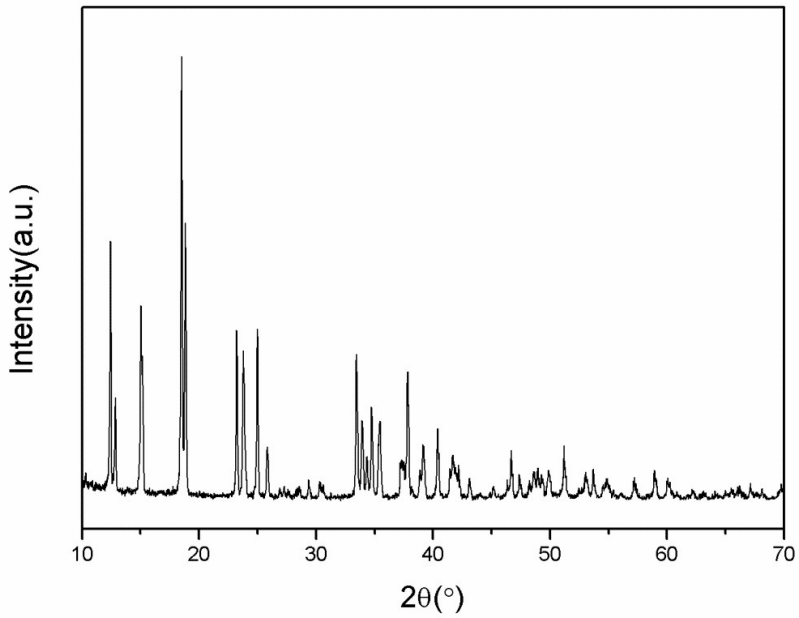

Fig. S1 shows XRD patterns of the resulting $Ce[Co(CN)_6]$, which is similar to $La[Co(CN)_6]$.

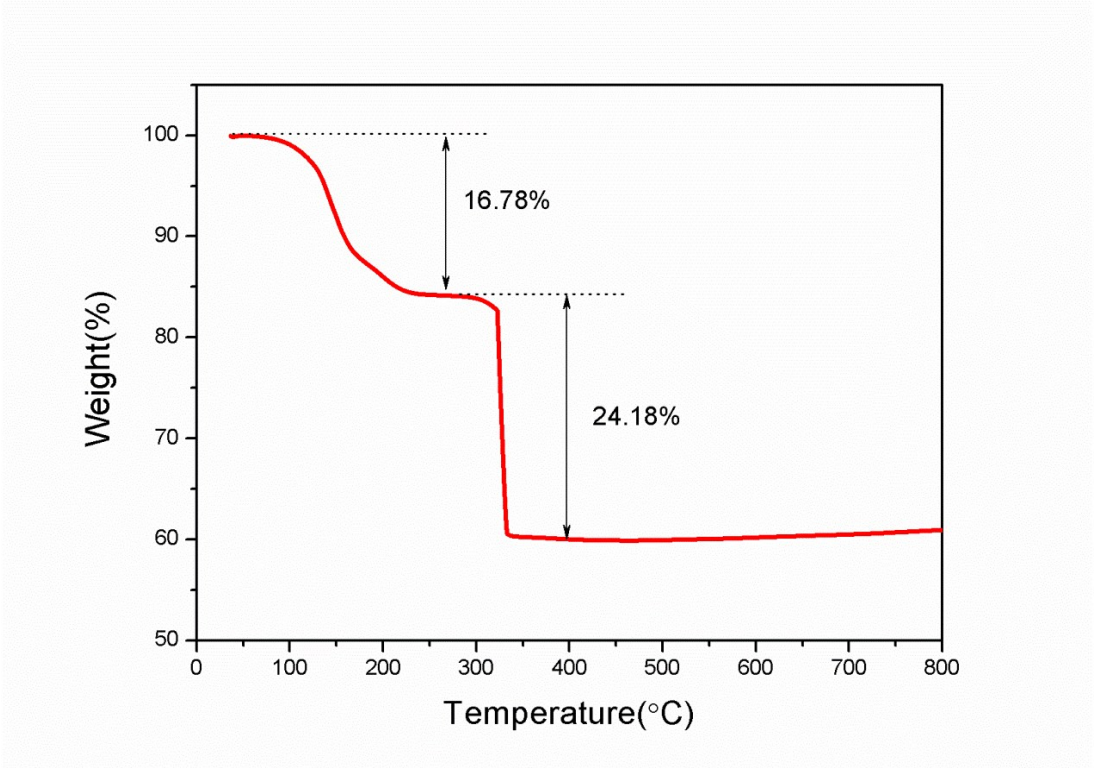

Fig. S2 TGA curves of the $Ce[Co(CN)_6]$.

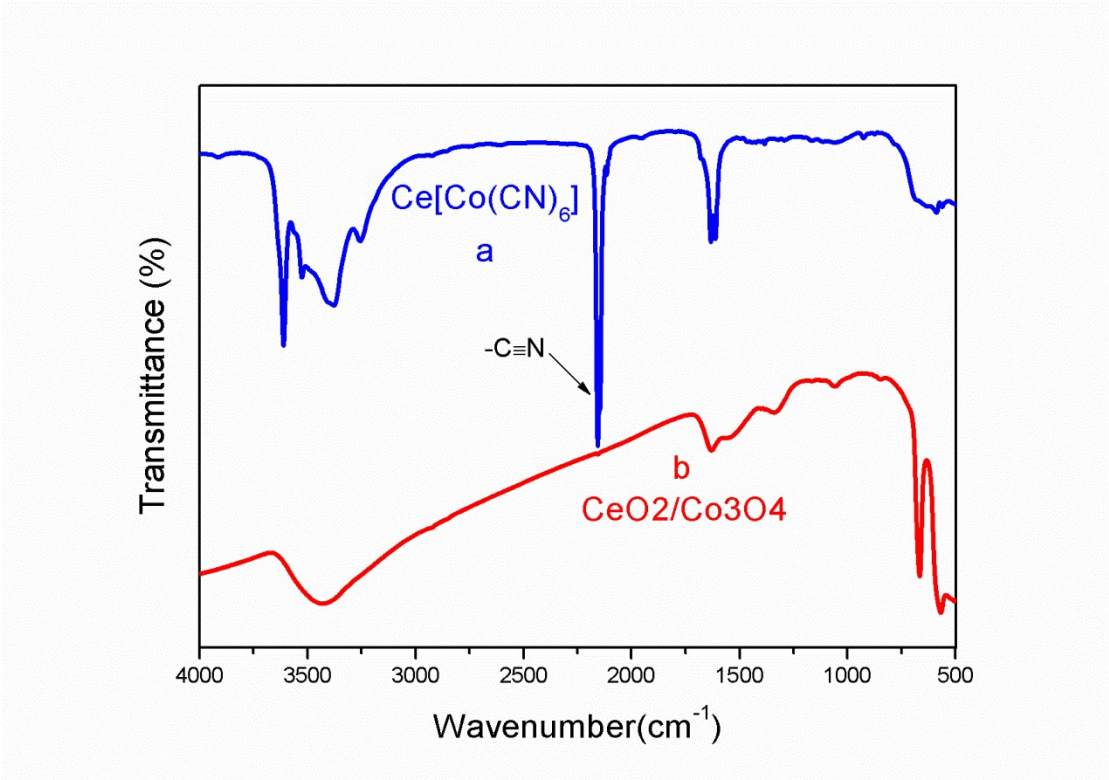

Fig. S3 FTIR spectra of (a) the $Ce[Co(CN)_6]$ precursor and (b) the CeO_2/Co_3O_4 nanojunctions.

Fig. S3 shows the FTIR spectra of the $Ce[Co(CN)_6]$ precursor and the CeO_2/Co_3O_4 nanojunctions, respectively. The FTIR spectrum of the $Ce[Co(CN)_6]$ precursor exhibits a dominant peak at 2158 cm^{-1}, which is attributed to -C≡N- stretching vibration. The characteristic peak at 1610 cm^{-1} arises from C=O stretching of the poly(vinylpyrrolidone) (PVP) amide unit[7] and the peak located at 3386 cm^{-1} is related to the ν(O–H) of the crystal water[8]. As we can see from the FTIR spectrum of the CeO_2/Co_3O_4 nanojunctions, the peak of -C≡N- stretching vibration disappears, indicating MOF has been totally decomposed during the annealing process, that is to say, there is no MOF residual in the as-prepared CeO_2/Co_3O_4 nanojunctions. And the peak located at 3430 cm^{-1} is possibly attributed to the hydroxyl groups in the sample or absorbed water molecules[9], which is consistent with the results of XPS (Fig. 3a).

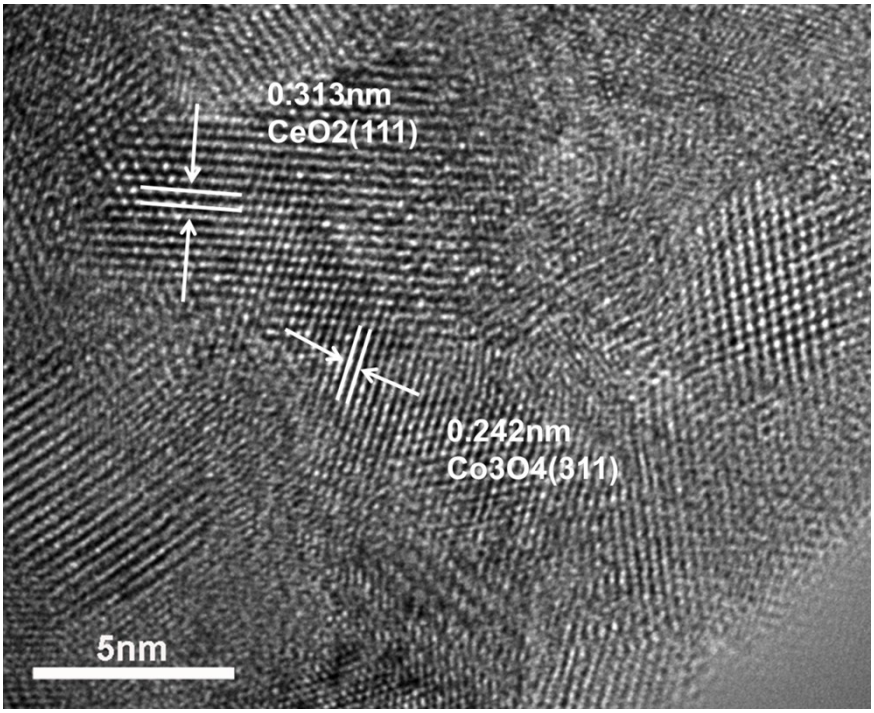

Fig. S4 HRTEM image of the porous CeO_2/Co_3O_4 nanojunctions.

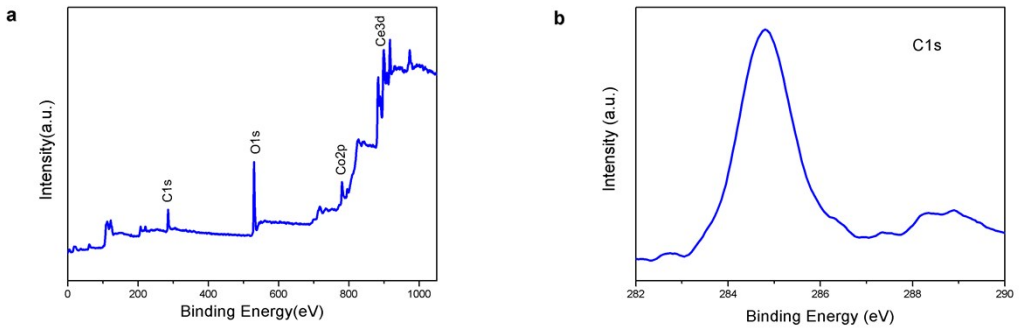

Fig. S5 XPS spectra of the as-prepared porous CeO_2/Co_3O_4 nanojunctions: (a) survey spectrum, (b) C 1s binding energy spectrum.

The existence of C is possibly derived from carbonization of the -C≡N- linker in the MOF, and it can be also considered to be beneficial to avoid the aggregation of in situ generated nanometer-sized CeO_2/Co_3O_4 nanojunctions, which are uniformly distributed in the whole hexagonal structure.

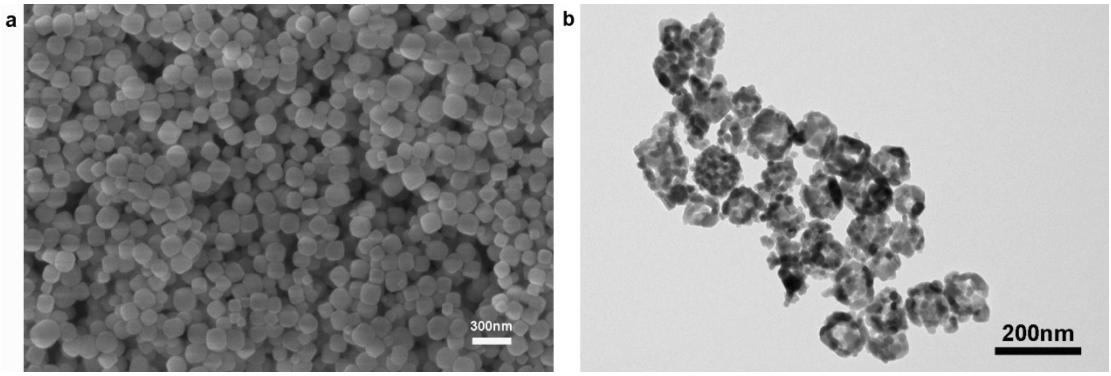

Fig. S6 (a) SEM image of the $Co_3[Co(CN)_6]_2$, (b)TEM image of pure Co_3O_4

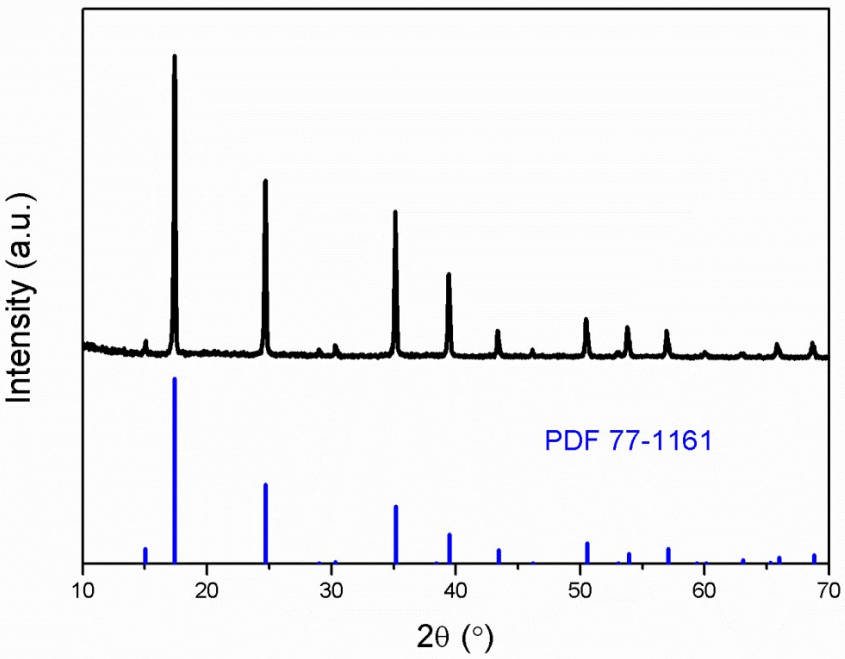

Fig. S7 The XRD pattern of $Co_3[Co(CN)_6]_2$

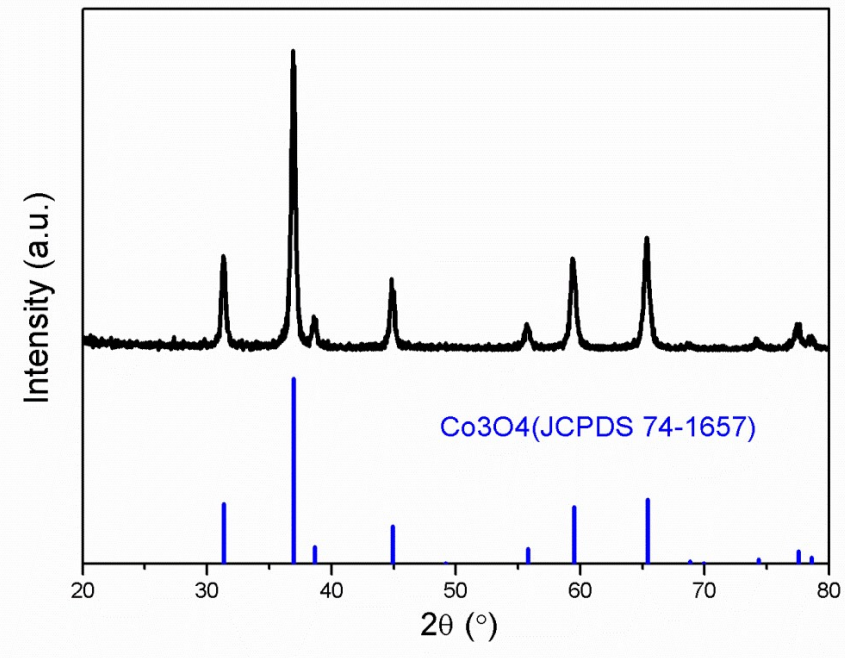

Fig. S8 The XRD patterns of pure Co_3O_4.

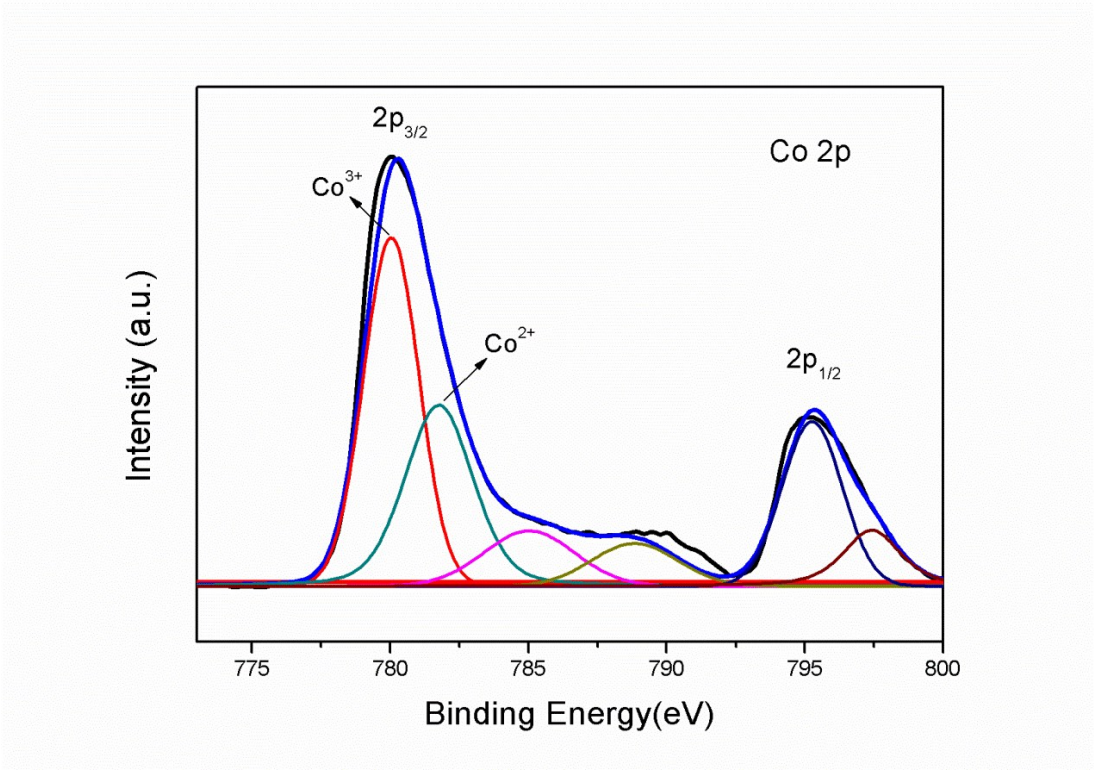

Fig. S9 Co 2p binding energy spectrumofpure Co_3O_4

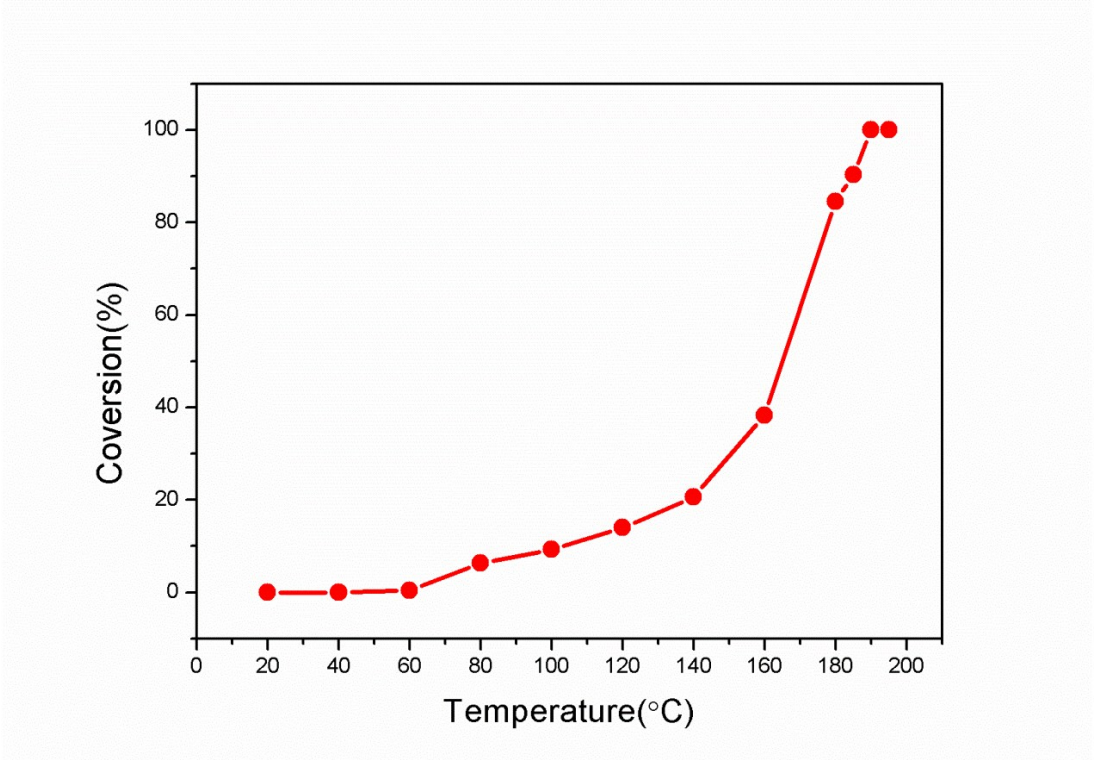

Fig. S10 Conversion as a function of temperature for CO oxidation over rare Co_3O_4.

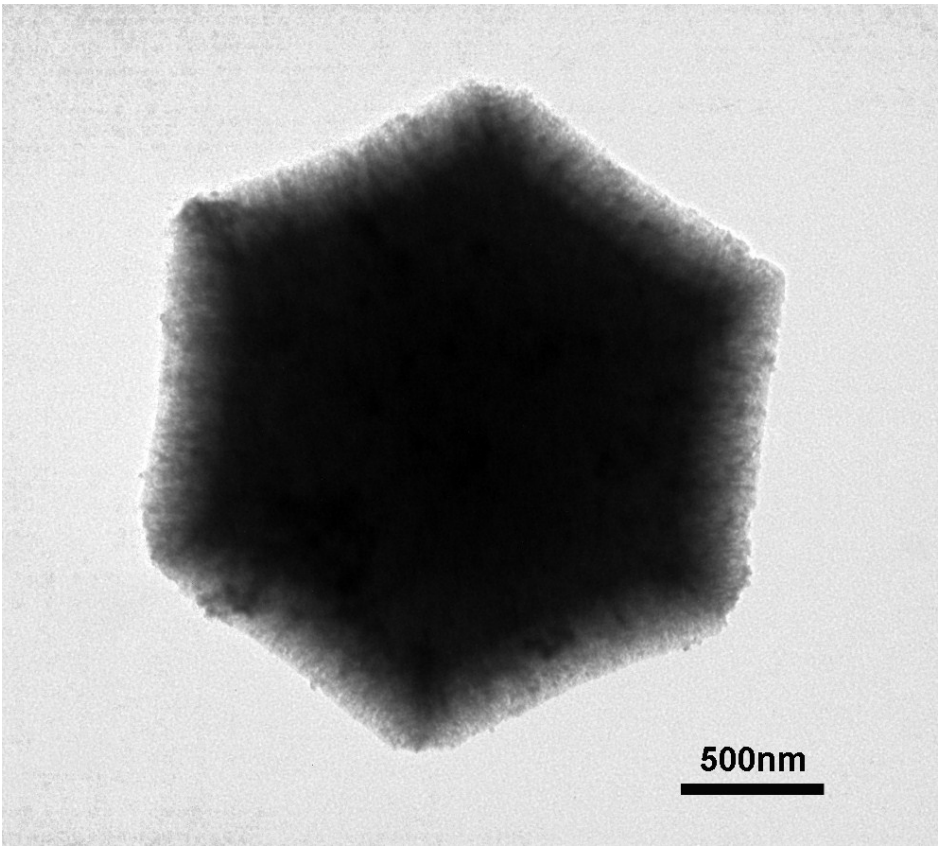

Fig. S11 The TEM image of porous CeO_2/Co_3O_4nanojunctions after the CO oxidation test.

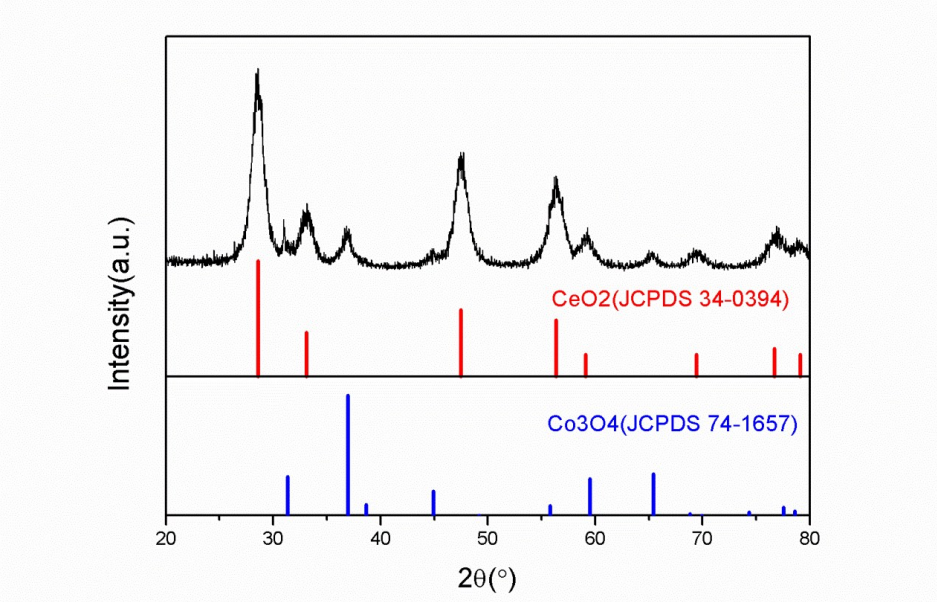

Fig. S12 The XRD pattern of porous CeO_2/Co_3O_4 nanojunctions after the CO oxidation test.

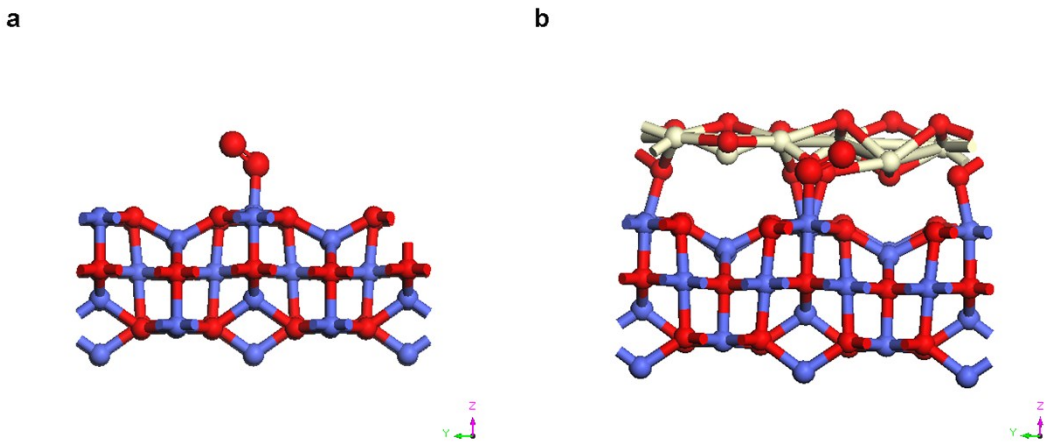

Fig. S13 Schematic structure of O_2 adsorbed on (a) the Co_3O_4 (110) surface and (b) the interface of CeO_2/Co_3O_4.

Table S1 The comparison of the catalytic properties for CO oxidation of some related catalysts and our porous CeO_2/Co_3O_4nanojunctions.

catalysts	**CO/%**	**T_{100}/℃**	**Reference**
porous CeO_2/Co_3O_4nanojunctions	1	110	This work
Co_3O_4@CeO_2nanowire	1	160	Nano Research, 2015, 8(6): 1944-1955.
Co_3O_4@CeO_2 cubes	1	190	Chem. Eur. J. 2014, 20, 4469–4473
$ZnCo_2O_4$@CeO_2 spheres	1	200	ACS Appl. Mater. Interfaces 2014, 6, 22216 − 22223
CeO_2-ZnO composite hollow microsphere	0.5	300	ACS Appl. Mater. Interfaces 2014, 6, 421 − 428
CeO_2 nanorods	1	292	J. Mater. Chem. A 2014, 2, 16459–16466
CeO_2 -ZnO	1	260	Materials Letters 2016, 181, 161–

Table S2 The comparison of the catalytic properties for CO oxidation of our porous CeO_2/Co_3O_4nanojunctions with some noble metals.

catalysts	CO/%	T_{100}/℃	Reference
porous CeO_2/Co_3O_4nanojunctions	1	110	This work
Pt@C/SiO_2	1	138	Carbon, 2016, 101, 324-330.
Pd/ZnO	1	160	Nano Res. 2011, 4(1): 83–91
Pd-TiO_2	1	>200	Progress in Natural Science: Materials International, 2016.

Table S3 The comparison of O-O bond length for O_2 molecule and adsorbed O_2 on the Co_3O_4 (110) surface and the interface of CeO_2/Co_3O_4 nanojunctions.

	O_2	Co_3O_4 (110)-O_2	CeO_2/Co_3O_4-O_2
O-O bond length[Å]	1.236	1.282	1.287

References

1. G. Kresse and J. Furthmüller, *Phys. Rev. B*, 1996, **54**, 11169.
2. G. Kresse and J. Hafner, *Phys. Rev. B*, 1993, **48**, 13115.
3. P. E. Blöchl, *Phys. Rev. B*, 1994, **50**, 17953.
4. G. Kresse and D. Joubert, *Phys. Rev. B*, 1999, **59**, 1758.
5. M. P. Teter, M. C. Payne and D. C. Allan, *Phys. Rev. B*, 1989, **40**, 12255.
6. J. P. Perdew, K. Burke and M. Ernzerhof, *Phys. Rev. Lett.*, 1996, **77**, 3865.
7. L. Hu, N. Yan, Q. Chen, P. Zhang, H. Zhong, X. Zheng, Y. Li and X. Hu, *Chem. Eur. J.*, 2012, **18**, 8971-8977.
8. F. Zheng, D. Zhu, X. Shi and Q. Chen, *J. Mater. Chem. A*, 2015, **3**, 2815-2824.
9. K. Babitha, A. Sreedevi, K. Priyanka, B. Sabu and T. Varghese, *Indian J. Pure Appl. Phys.*, 2015, **53**, 596-603.